

1 **A Phytochrome B-PIF4-MYC2 Module Tunes Secondary Cell Wall**
2 **Thickening in Response to Shaded Lighting**

3

4 Fang Luo^{1,2,7}, Qian Zhang^{1,2,7}, Hu Xin^{1,3}, Hongtao Liu¹, Hong-Quan Yang⁴, Monika S
5 Doblin^{5,6}, Antony Bacic^{5,6} and Laigeng Li^{1*}

6 ¹ National Key Laboratory of Plant Molecular Genetics, CAS Center for Excellence in
7 Molecular Plant Sciences, Chinese Academy of Sciences, Shanghai 200032, China

8 ² University of the Chinese Academy of Sciences, Beijing 100049, China

9 ³ Key Laboratory of Biodiversity Conservation in Southwest, State Forestry
10 Administration, Southwest Forestry University, Kunming 650224, China

11 ⁴ College of Life and Environmental Sciences, Shanghai Normal University, Shanghai
12 200234, China.

13 ⁵ La Trobe Institute for Agriculture and Food, School of Life Sciences, Department of
14 Animal, Plant and Soil Sciences, AgriBio, La Trobe University, Bundoora VIC 3086,
15 Australia

16 ⁶ Sino-Australia Plant Cell Wall Research Centre, State Key Laboratory of Subtropical
17 Silviculture, School of Forestry and Biotechnology, Zhejiang A&F University,
18 Hangzhou 311300, China

19

20 ⁷ These authors contributed equally to this work.

21

22 *Corresponding author: Laigeng Li, e-mail: lgli@cemps.ac.cn; Tel:
23 +86-021-54924151

24

25 Short title: Shade inhibition of secondary cell wall thickening.

26

27

28

29 **Abstract**

30 Secondary cell walls (SCW) in stem xylem cells provide mechanical strength and
31 structural support for growth. SCW thickening is light- regulated and varies under
32 different light growth conditions. Our previous study revealed that blue light enhances
33 SCW thickening through the activity of MYC2 directed by CRYPTOCHROME1
34 (CRY1) signaling in stem xylary fiber cells. In this study, we demonstrate that the low
35 ratio of red: far-red light (R:FR) of the shaded light condition inhibits SCW
36 thickening in the inflorescence stem of *Arabidopsis*. Phytochrome B (PHYB) plays a
37 dominant role in perceiving the R:FR balance. Under white and red-light conditions,
38 *phyB* mutants display thinner SCWs in xylary fibers, but thicker SCWs are deposited
39 in the PHYTOCHROME INTERACTING FACTORS (PIFs) quadruple mutant
40 *pif1pif3pif4pif5* (*pifq*), suggesting involvement of the PHYB-PIFs signaling module in
41 regulating SCW thickening. Interaction of PIF4 with MYC2 affects MYC2
42 localization in nuclei and inhibits its transactivation activity on the *NST1* promoter.
43 Shade conditions mediate the PIF4 interaction with MYC2 to regulate SCW
44 thickening. Genetic analysis confirms that the regulation of SCW thickening by *PIFs*
45 is dependent on *MYC2* function. Together, these data reveal a molecular mechanism
46 for the effect of shaded light inhibition on SCW thickening in stems of *Arabidopsis*.

47

48

49

50 **Introduction**

51 In higher plants, all cells are encased in a primary cell wall laid down during cell
52 elongation that is flexible (to allow growth) yet possesses sufficient tensile strength to
53 withstand the turgor pressure that drives growth. The primary cell wall defines the
54 shape of a plant cell and is important for communication between plants and their
55 environment(Doblin et al., 2010). Some types of specialized cells such as fiber and
56 vessel cells in stem xylem deposit a rigid secondary cell wall (SCW) inside the
57 primary cell wall after cell elongation has ceased, which provides plants with the
58 mechanical strength to withstand enormous compressive forces and the capacity to
59 transport water to aerial organs(Zhong and Ye, 2015). During plant growth, the plant
60 body is built and structured primarily by conversion of photosynthetic products into
61 SCW. The main components of lignified SCW include cellulose, hemicelluloses and
62 lignin, with deposition of lignin being a sign of SCW thickening. Expression of SCW
63 biosynthesis genes is controlled by a hierarchy of transcriptional regulatory networks.
64 *SND1/NST1* and *VND6/VND7* are key regulators at the top tier of the regulatory
65 network that specifically control SCW formation in fiber and vessel cells, respectively,
66 in *Arabidopsis*(Zhong et al., 2010; Taylor-Teeple et al., 2015).

67 In addition to developmental signals, various external environmental cues, including
68 light, water and temperature, affect SCW formation(Le Gall et al., 2015). Light
69 induces a range of effects on plant cell wall formation(Le Gall et al., 2015). For
70 example, when grown under blue light, *Arabidopsis* deposits a mechanically
71 strengthened inflorescence stem due to a thickening of the SCW of fiber cells. It was
72 demonstrated that the blue light signal induces *MYC2* expression which activates
73 *NST1* expression by binding to its promoter, leading to an enhancement of SCW
74 thickening(Zhang et al., 2018a). However, under shaded light conditions with a lower
75 ratio of red to far-red (R:FR) light, plants exhibit an increase of cell elongation and a
76 subsequent reduction in their SCW thickening(Sasidharan et al., 2008; Sasidharan et
77 al., 2010; Casal, 2012; Pedmale et al., 2016; Wu et al., 2017). The molecular
78 mechanism underlying this reduction of SCW thickening caused by shaded light

79 conditions remains unknown.

80 The red/far-red photoreceptor, phytochrome B (PHYB) exists in two forms that are
81 reversibly interconvertible by perceiving red and far-red light(Quail, 1991). The Pr
82 form of PHYB absorbs red light to rapidly revert to the Pfr form which absorbs
83 far-red light to return to the Pr form(Franklin, 2008). In response to the R:FR ratio
84 signal, interconversion of the PHYB Pr-Pfr forms activates downstream molecular
85 pathways to regulate induction of seed germination, seedling de-etiolation, shade
86 avoidance, and floral initiation(Franklin and Quail, 2010; Strasser et al., 2010).

87 Red light activates PHYB to interact with PHYTOCHROME INTERACTING
88 FACTORs (PIFs, mainly a quartet of members: PIF1, PIF3, PIF4, and PIF5), leading
89 to their degradation(Bauer et al., 2004; Monte et al., 2004; Al-Sady et al., 2006; Shen
90 et al., 2007; Lorrain et al., 2008), whereas far-red light inactivates PHYB and
91 stabilizes PIFs, inducing stem elongation and other morphogenesis
92 processes(Hornitschek et al., 2012; Leivar et al., 2012). However, how PHYB
93 responds to the R:FR ratio in regulation of the SCW thickening is largely unknown.

94 The transcription factor (TF) MYC2 is considered a transcriptional regulatory “hub”
95 interconnecting a variety of biological processes(Kazan and Manners, 2013). MYC2
96 interacts with different TFs to integrate the crosstalk among different signaling
97 pathways including jasmonate (JA)-mediated pathogen defences, abscisic acid (ABA),
98 ethylene, gibberellic acid (GA) and light signals(Chen et al., 2012; Hong et al., 2012;
99 Song et al., 2014). The blue light signal upregulates expression of *MYC2* which then
100 activates the *NST1*-mediated SCW thickening by direct binding to the *NST1*
101 promoter(Zhang et al., 2018a). Here, we show that the low R:FR ratio of a shaded
102 light condition inhibits SCW thickening in *Arabidopsis* inflorescence stems. Our
103 analyses indicated that the R:FR light is perceived by PHYB to alter the status of PIF4,
104 which act as a direct regulator of MYC2 to modulate SCW thickening. This study
105 reveals a molecular pathway of the SCW thickening in response to R:FR ratio light
106 conditions.

107

109 **Results**

110 **Light R:FR ratio affects SCW thickening in the inflorescence stem of *Arabidopsis***

111 As our previous study showed that a blue light signal enhances SCW thickening in
112 *Arabidopsis* inflorescence stems(Zhang et al., 2018a), we were interested in further
113 examining the effect of light with a lower ratio of R:FR, which imitates shaded light
114 conditions, on SCW thickening during inflorescence stem growth. First, wild-type
115 (WT) plants were grown in normal white light (WL) conditions to bolting. When the
116 inflorescence stem started to grow, plants were transferred to light conditions with a
117 different R:FR ratio and the growth of the inflorescence stem monitored. The
118 inflorescence stem grew much faster (**Figure 1, A and B**) and had a significantly
119 lower tensile strength (**Figure 1C**) under white light supplemented with far-red light
120 (FR) (WL+FR) compared to white light (WL). This shows that the low R:FR ratio
121 condition affected both inflorescence stem growth and mechanical strength.
122 Anatomical analyses of the stem structure revealed that the SCW thickness in fiber
123 cells was significantly decreased, but vessel cell SCW thickness showed little
124 difference (**Figure 1, D and E**). Expression of the SCW thickening marker genes
125 (*NST1*, *SND1*, *4CLI* and *IRX8*)(Lee et al., 1997; Zhong et al., 2006; Mitsuda et al.,
126 2007; Hao et al., 2014) were down-regulated under low R:FR conditions
127 (**Supplemental Figure S1**). Content of lignin and crystalline cellulose, the typical
128 SCW components, was significantly lower under low R:FR condition (**Figure 1, F**
129 **and G**). These data suggest that the additional far-red light promotes stem elongation
130 and inhibits SCW thickening in stem fiber cells.

131

132 **PHYB and PIFs are involved in regulating cell elongation and SCW thickening**
133 **in *Arabidopsis* inflorescence stem**

134 R/FR light is perceived by the photoreceptor PHYB which induces a series of
135 responses through PIF proteins(Reed et al., 1993; Pham et al., 2018). To dissect the
136 genetic base of the light R:FR ratio effect on SCW thickening, we analyzed the
137 inflorescence stem growth of *phyB* and quadruple *pif1pif3pif4pif5* (*pifq*) mutants.

138 *phyB* mutants displayed a lodging phenotype and grew longer inflorescence stems
139 than wild-type (WT), while *pifq* mutants showed erect growth with shorter
140 inflorescence stems compared to WT (**Figure 2, A and B; Supplemental Figure**
141 **S2A**). Stem elongation growth was determined by measuring the distance between
142 two markers on the inflorescence stem during its growth process. The elongation
143 growth was increased in *phyB* but decreased in *pifq* mutant plants (**Figure 2C**). The
144 inflorescence stem mechanical properties, measured as tensile strength, were also
145 significantly impacted: *phyB* inflorescence stems had decreased tensile strength,
146 whereas the tensile strength of *pifq* mutant inflorescence stems was increased (**Figure**
147 **2G**). To analyze the cell length and cell wall structure in the inflorescence stem, the
148 stem was disintegrated to measure the length of xylem fibers which are the
149 predominant cell type in mature inflorescence stems. The fiber cells of *phyB* plants
150 were longer whereas those of *pifq* plants were shorter than those in WT (**Figure 2D;**
151 **Supplemental Figure S2B**).

152 Meanwhile, cross-sections of the stem showed a difference in the cell wall thickness
153 in interfascicular fiber cells (**Figure 2F; Supplemental Figure S2C**). Compared to
154 WT, cell wall thickness in interfascicular fiber cells was decreased in *phyB* but
155 increased in *pifq* plants, whereas the thickness of vessel cells was unaltered (**Figure 2,**
156 **E and F**). Furthermore, both the lignin and crystalline cellulose content was
157 decreased in *phyB* but increased in *pifq* plants (**Figure 2, H and I**, respectively).

158 In parallel with the knock-out mutant analyses, *Arabidopsis* plant overexpressing
159 *PHYB* (*PHYB-OE*) and *PIF4* (*PIF4-OE*) were also generated, and their inflorescence
160 stem properties analyzed. *PHYB-OE* transgenics had shorter and stronger (increased
161 tensile strength) inflorescence stems while those of *PIF4-OE* plants were thinner and
162 weaker (**Supplemental Figure S3; Figure 3C**). Examination of stem cross-sections
163 indicated that *PHYB* overexpression resulted in thicker cell walls in xylary
164 interfascicular fiber cells while *PIF4* overexpression led to thinner fiber cell walls
165 relative to WT (**Figure 3, A and B**). Lignin and crystalline cellulose content was
166 increased in the *PHYB-OE* inflorescence stems but decreased in *PIF4-OE* stems
167 (**Figure 3, D and E**). In contrast, the cell wall thickness of vessel cells was largely

168 unaffected in *PHYB-OE* but was decreased in *PIF4-OE* plants (**Figure 3, A and B**).
169 Transcriptional analyses of the SCW thickening genes (*NST1*, *SND1*, *4CLI* and *IRX8*)
170 demonstrated that the expression of these genes was upregulated in *PHYB-OE* plants
171 but suppressed in *PIF4-OE* plants (**Figure 3F**). These results indicate that SCW
172 thickening is positively regulated by *PHYB* but negatively regulated by *PIFs* in
173 inflorescence stem xylary fibers.

174

175 **MYC2 links the *PHYB-PIFs* signal module to SCW thickening**

176 As shown above, SCW thickening is genetically regulated by *PHYB* and *PIFs* and
177 also conditionally modified by light R:FR ratio. Next, we examined whether the effect
178 of *PHYB* and *PIFs* is dependent on the red-light signal. *phyB* and *pifq* mutants were
179 grown under red light (high R:FR). The inflorescence stem of *phyB* mutant plants
180 showed a significant decrease of the stem tensile strength, SCW thickening was
181 severely impacted in fiber cells, but was essentially unchanged in vessel cells (**Figure**
182 **4, A-C**). Conversely, the *pifq* mutants displayed increased stem tensile strength,
183 accumulated much thicker SCWs in xylary fiber cells and had a modest increase in
184 vessel cells, compared to those in WT plants (**Figure 4, A-C**). Lignin content was
185 decreased in the *phyB* mutant but increased in the *pifq* mutant (**Figure 4D**). Consistent
186 with these findings, the expression of the SCW thickening genes (*NST1*, *SND1*, *4CLI*
187 and *IRX8*) was downregulated in the *phyB* mutant but upregulated in the *pifq* mutant
188 (**Figure 4E**). These data suggest that high R:FR facilitates SCW thickening through
189 *PHYB*-enhanced SCW gene expression, while *PIFs* inhibit this process. Analysis of
190 gene expression showed that *PHYB* and *PIF* quadruple members are both expressed in
191 inflorescence stems, and among them *PIF4* and *PIF5* have the highest abundance
192 (**Supplemental Figure S4A**). Also, *PIF4* promoter-GUS analysis indicated its
193 expression in interfascicular fiber cells (**Supplemental Figure S4B**).

194 Next, we dissected the molecular pathway that mediates the *PHYB-PIFs* signal to
195 SCW thickening. Five-week-old WT plants at the stage of inflorescence stem
196 elongation were moved from normal light to dark for 24 h in order to shut-down the
197 light-induced gene expression, and then transferred to red light (high R:FR)

198 conditions for 2 h. Stem samples were collected for RNA-sequencing (see
199 **Supplemental Figure S5A**). Compared to 24 hours of dark status, a group of 2,203
200 differentially expressed genes (DEGs) were detected after red-light treatment, among
201 which two thirds were up-regulated while one third were down-regulated
202 (**Supplemental Table S1; Supplemental Figure S4B**). The regulated genes included
203 red light responsive photopigment genes (*PSY*, *PORC*, *GUN5*) and target genes of
204 PIFs (*PIL1*, *ATHB2*, *BBX28*)(Zhang et al., 2013; Toledo-Ortiz et al., 2014), indicative
205 of the red-light signaling effectiveness. It was noticed that the expression of cell
206 expansion genes (*XTH22*, *XTH27*, *XTH30*, *EXPA1*) was inhibited, but the SCW
207 thickening-related regulatory genes, including *NST1* and *MYC2*, were up-regulated in
208 response to red light (**Supplemental Figure S5C**)(Matsui et al., 2005; Claisse et al.,
209 2007; Goh et al., 2012; Taylor-Teeple et al., 2015). Interestingly, expression of
210 *VND6/VND7* which control vessel SCW thickening was not induced by red light
211 (**Supplemental Table S1**). The red-light induction of *NST1*, *MYC2* and other key
212 genes for SCW thickening was further confirmed in RT-qPCR analysis
213 (**Supplemental Figure S6**). Conversely, when exposed to far-red light conditions,
214 *MYC2* and *NST1* expression was inhibited in WT plants, however, the inhibition was
215 reduced in *phyB* and *pifq* mutants (**Supplemental Figure S7**). These results suggest
216 that the expression of *MYC2* is induced by red light and inhibited by far-red light and
217 regulated through PHYB and PIFs.

218

219 **PIF4 affects MYC2 stability and inhibits its transcriptional activity.**

220 It is known that *MYC2* binds to the *NST1* promoter to regulate SCW
221 thickening(Zhang et al., 2018a). To analyze how PIFs affect *MYC2* function in SCW
222 thickening, we conducted a dual-luciferase (LUC) reporter assay in *Arabidopsis*
223 protoplasts. We co-expressed PIFs with *MYC2* to check the *MYC2* transcriptional
224 activity on the *NST1* promoter. *MYC2*, but neither PIF4 nor PIF5, were able to
225 activate the *NST1* promoter (**Figure 5, A and B**). When *MYC2* was co-expressed with
226 either PIF4 or PIF5, the *MYC2* activity on the *NST1* promoter was reduced (**Figure**
227 **5B**), suggesting that the *MYC2* transcriptional activity is repressed by either PIF4 or

228 PIF5. Studies have shown an interaction between PIFs and MYC2 to contribute to
229 apical hook formation and plant defense(Zhang et al., 2018b; Zhao et al., 2021). Our
230 yeast two-hybrid assays verified the PIF4 interaction with MYC2 is likely through the
231 PIF4 N-terminal region (**Supplemental Figure S8**).

232 Then, the subcellular localization of MYC2, its homolog MYC4 and PIF4 was
233 examined. Tobacco leaf cells were employed to express MYC2/MYC4-YFP and
234 PIF4-CFP proteins and then treated with dark condition. When expressed separately,
235 PIF4 and MYC2/MYC4 proteins were localized in the nucleus as distinct dots.
236 However, when PIF4 and MYC2/MYC4 were co-expressed together, the nuclear
237 localization of PIF4 was unchanged, whereas MYC2 and MYC4 became distributed
238 throughout the nucleus (**Figure 5B**). These results suggest that PIF4 affects
239 MYC2/MYC4 nuclear localization and/or stability.

240 Next, MYC2 protein stability was tested in *planta*. MYC2-YFP was expressed in
241 wild-type and *pifq* mutant plants. Immunoblot analysis showed that the MYC2
242 abundance in inflorescence stems was decreased in both dark and in far-red light
243 conditions, while MYC2 is more stable in the *pifq* mutant plants compared to the WT
244 background (**Figure 6, A and B**). Furthermore, the MYC2-YFP fluorescence signal in
245 root tip cells showed a substantial decrease in the WT background after dark treatment,
246 but the reduction was attenuated in the *pifq* mutant background (**Figure 6C**). These
247 results suggest that PIFs affect MYC2 protein stability.

248

249 **MYC2/MYC4 act downstream of PHYB and PIFs in a genetic pathway to**
250 **regulate stem SCW thickening.**

251 Next, *myc2myc4* double mutants were crossed with *pifq* and *phyB* mutants to test
252 whether MYC2 lies in the same genetic pathway to PHYB and PIFs in the regulation
253 of SCW thickening. The *pifq* phenotype of a shorter inflorescence stem relative to WT
254 (**Figure 2, A and B**) was restored in the sextuple *pifqmyc2myc4* mutant under white
255 light (**Figure 7, A and B**). Consistently, both fiber cell thickness (**Figure 7, C and D**)
256 and expression of the SCW thickening related genes such as *NST1*, *4CL1*, and *IRX8*
257 were decreased in *pifqmyc2myc4* plants compared with *pifq* (**Figure 7, E and F**).

258 Furthermore, rosette leaf growth and hypocotyl elongation, which were inhibited in
259 *pifq*(Leivar and Quail, 2011), was partly rescued in *pifqmyc2myc4* plants
260 (**Supplemental Figure S9, A and D and E**). These results indicate that *MYC2/MYC4*
261 are genetically downstream of the *PHYB-PIFs* signaling module. Nevertheless, the
262 faster elongating-stem and thinner-SCW phenotypes of *phyB* mutants were enhanced
263 in *phyBmyc2myc4* triple mutants (**Figure 7, A-D**), and the SCW regulatory and
264 biosynthesis-related gene expression was slightly down-regulated in triple mutants
265 compared with *phyB* (**Figure 7E**). Additionally, *phyBmyc2myc4* mutants exhibited
266 greater hypocotyl elongation than *phyB* seedlings (**Supplemental Figure S9, B and**
267 **C**). Together, these data indicate that the *PHYB-PIFs* signaling module regulates SCW
268 thickening in the inflorescence stem of *Arabidopsis*. *MYC2* acts downstream of *PIFs*
269 to modify the transcription networks of SCW thickening to tune plant stem growth.

270

271

272 **Discussion**

273 **Shaded light promotes cell elongation as well as inhibits SCW thickening in**
274 **inflorescence stem of *Arabidopsis***

275 In the xylem of the plant vascular system, fiber and vessel cells develop a thickened
276 SCW to provide mechanical support and facilitate water transport(Lucas et al., 2013).
277 SCW thickening in xylem cells is regulated by growth and developmental cues as
278 well as environmental conditions through a combination of hormone and
279 mechano-sensing signals(Didi et al., 2015; McCahill and Hazen, 2019; Hori et al.,
280 2020). Plants grow longer petioles and inflorescences with weak stem strength and
281 thinner SCW under shade conditions(Kozuka et al., 2010; Casal, 2012; Wu et al.,
282 2017), but the mechanisms of how the shaded light modulates SCW thickening and
283 mechanical properties are largely unknown.

284 A characteristic feature of a shaded light condition is the decreased red:far-red (R:FR)
285 light ratio(Hersch et al., 2014). Using the *Arabidopsis* inflorescence stem as a model,
286 we examined the effect of the R:FR ratio on the SCW thickening of interfascicular
287 fibers and vessel cells, the major cell types with SCW. A low ratio of R:FR light
288 induced rapid elongation of the inflorescence stem resulting in a lodging phenotype
289 (**Figure 1, A and B**), consistent with the reported shaded light effect on stem
290 growth(Casal, 2012), indicating that the low ratio of red:far-red light can be used as
291 an experimental proxy to simulate shaded light conditions. Anatomical analyses
292 reveal that the shaded light results in plants with a thinner SCW in stem fiber cells,
293 and weaker mechanical strength of the inflorescence stem (**Figure 1, A and C-E**).
294 Expression of SCW regulatory and biosynthesis-related genes is down-regulated
295 (**Supplemental Figure S1**). Many plants respond to low R:FR ratio light with the
296 shade avoidance syndrome (SAS), displaying a series of well described
297 morphological changes such as enhanced elongation of hypocotyl, internode and
298 petiole(Liu et al., 2021). In contrast, the cellular and molecular mechanisms
299 underpinning these morphological phenotypes to a low R:FR ratio light have not been
300 well defined. Plant morphogenesis and body structure is defined by the assembly and

301 architecture of the cell wall(Huang et al., 2018). Our study shows that SCW
302 thickening, and cell elongation are coordinated and tightly regulated by shaded light
303 conditions.

304

305 ***PHYB-PIFs* signaling module mediates regulation of SCW thickening in**
306 **inflorescence stem of *Arabidopsis*.**

307 The *PHYB-PIFs* signaling module plays a primary role in plant SAS and
308 morphogenesis through *PHYB-PIFs*-controlled gene expression(Reed et al., 1993;
309 Pham et al., 2018). Shaded light inactivates *PHYB* and subsequently diminishes its
310 action on the degradation of *PIFs*, leading to regulation of the downstream genes to
311 modulate plant growth(Lorrain et al., 2008; Jia et al., 2020). Whether *PHYB* and *PIFs*
312 are directly involved in the shaded light inhibition of SCW thickening is unresolved.
313 To answer this question, *PHYB* and *PIFs* function on cell wall formation of
314 inflorescence stem was examined. *phyB* and *pifq* mutants have contrasting phenotypes
315 of SCW thickening and mechanical strength properties in inflorescence stem (**Figure**
316 **2 and 3**), indicating that the SCW thickening process is positively regulated by *PHYB*
317 but negatively regulated by *PIFs*.

318 In *Arabidopsis* inflorescence stems, SCW formation in the fiber and vessel cells are
319 initiated under the control of the master TF switches of *NST1/SND1*(Zhong et al.,
320 2006; Mitsuda et al., 2007) and *VND6/VND7*(Yamaguchi et al., 2010), respectively.
321 *NST1/SND1* and *VND6/VND7* regulate several downstream genes in controlling SCW
322 thickening(Taylor-Teeple et al., 2015) through highly cell-type specific
323 spatio-temporal regulation modulated through distinct regulatory signals(Zhong et al.,
324 2006; Zhong et al., 2008). In this study, low R:FR ratio results in thinner SCW in
325 interfascicular fiber cells of inflorescence stems while the vessel SCW were largely
326 unaffected (**Figure 1, D and E**). Genetic evidence reveals that the *PHYB-PIFs*
327 interaction mediates the signaling underlying the low R:FR ratio inhibition of SCW
328 thickening in fiber cells but not in vessel cells (**Figure 2**). Interestingly, the blue light
329 signal dramatically affects SCW thickening in fiber cells with little effect on vessel
330 cells(Zhang et al., 2018a). Information from RNA sequencing indicated that

331 expression of *VND6/VND7* does not respond to red-light induction (**Supplemental**
332 **Table S1**). Therefore, light-induced SCW thickening appears to be through the
333 transcriptional network directed by *NST1* in fiber rather than xylem cells.

334

335 **Shaded light inhibits SCW thickening through PIF4 inactivation of MYC2**
336 **activity**

337 MYC2 interconnects a variety of environmental and developmental responses(Yadav
338 et al., 2005; Chen et al., 2012; Song et al., 2014). It is regulated at both transcriptional
339 and post-translational levels under various circumstances. Blue light induces the
340 expression of *MYC2* and *MYC4* and subsequently activates *NST1* to promote SCW
341 thickening(Zhang et al., 2018a). MYC2 protein is targeted for degradation during
342 hormone responses(Jung et al., 2015; Chico et al., 2020). In addition, MYC2 protein
343 is known to be destabilized under either dark or shade conditions, while red light
344 stabilizes MYC2 in a PHYB-dependent manner(Chico et al., 2014), indicating MYC2
345 plays a role in the light signaling pathway.

346 We demonstrate that *MYC2*, as well as the downstream expression of the SCW
347 thickening genes, are enhanced upon high R:FR light induction and reduced after a
348 far-red light treatment (**Supplemental Figure S5-7**). Meanwhile, MYC2 protein is
349 destabilized under far-red light and dark conditions in WT (**Figure 6, A and B**) but
350 more stable in the *pifq* mutant under the same treatments (**Figure 6, A and B**).
351 Therefore, we conclude that the *PHYB-PIFs* signaling module affects MYC2 protein
352 stability.

353 PIFs interact with MYC2 and such interaction plays a role in regulating the *NST1*
354 promoter transcriptional activity (**Figure 5, A and B**). MYC2/MYC4 activates *NST1*
355 transcription by binding its promoter, but PIF4 is inactive to *NST1* transcription.
356 MYC2/MYC4 and PIF4 are localized in nuclei as distinct dots (**Figure 5C**), similar to
357 that previously reported(Withers et al., 2012; Luo et al., 2014). However, when PIF4
358 and MYC2/MYC4 were co-expressed in the dark, PIF4 localization was unchanged,
359 whereas the dotted localization of MYC2 and MYC4 became distributed throughout
360 the nucleus (**Figure 5C**). This suggests that interaction of PIF4 with MYC2/MYC4

361 displaced MYC2 localization in the nucleus. It is known that low R:FR light condition
362 prevents PHYB from entering the nucleus and PIF4 becomes stable to interact with
363 other proteins(Chico et al., 2014; Leivar and Monte, 2014). In our study, PIF4
364 interacts with MYC2/MYC4 under shaded light conditions to either prevent
365 MYC2/MYC4 binding to the *NST1* promoter or induces MYC2 protein degradation,
366 leading to the inhibition of MYC2/MYC4 transcriptional activity. Given that PIF
367 proteins have been shown to be regulators of COP1 ubiquitination activity(Jang et al.,
368 2010) and that MYC2 protein abundance in *cop1* mutants is at a sustained high
369 level(Chico et al., 2014), it is possible that PIFs enhance MYC2/MYC4
370 polyubiquitination by COP1 to promote its degradation.

371 The interaction between PIF4 and MYC2/MYC4 in regulating SCW thickening was
372 further confirmed genetically by crossing *myc2myc4* with *pifq* and *phyB* mutants. By
373 analyzing the SCW phenotypes in inflorescence stem elongation growth (**Figure 7**),
374 we concluded that *MYC2* and *MYC4* function genetically downstream of *PHYB* and
375 *PIFs* to regulate SCW thickening in *Arabidopsis*. A recent study showed that
376 overexpression of *MYC2* in a *phyB* background partially suppressed its long
377 hypocotyl phenotype(Ortigosa et al., 2020), suggesting a genetic interaction of *PHYB*
378 and *MYC2* in hypocotyl elongation.

379 To summarize the findings of this study, we propose a model for the shaded light
380 inhibition of SCW thickening (**Figure 8**): Under normal light conditions (high R:FR
381 ratio), PHYB undergoes a light-dependent conformational change, which relieves the
382 interaction between chromophore-attachment domains and PAS-related domain
383 (PRD), and the nuclear-localization signal in the PRD is unmasked, enabling PHYB
384 to translocate to the nucleus and promote phosphorylation and degradation of PIF
385 proteins(Chen et al., 2005), thus resulting in MYC2/MYC4 stabilization and *NST1*
386 transcriptional activation to promote SCW thickening. Upon perception of shaded
387 light (low R:FR ratio), PHYB undergoes dark reversion from Pfr to its inactivated Pr
388 form, and returns to its cytoplasmic location since its nuclear-localization signal is
389 masked, allowing accumulation of PIFs in the nucleus where they interact with
390 MYC2/MYC4. Thus, the MYC2 activity on *NST1* transcription is inhibited, leading to

391 suppression of the SCW thickening (**Figure 8**). The study reveals a mechanism by
392 which shaded light inhibits SCW thickening.

393 Since regulation of SCW thickening is coordinated with cell elongation, our finding
394 that light signaling modules regulate SCW thickening has important implications for
395 both our understanding of plant growth and development and proffers a pathway to
396 begin to modify the mechanical properties of secondary cell walls that are crucial to
397 both forest (wood and wood product properties) and agricultural (crop improvement
398 through, for example, prevention of lodging) industries.

399

400

401

402

403

404

405

406 **Materials and methods**

407 **Plant materials and growth conditions**

408 The *Arabidopsis* wild-type (WT) ecotype used in this study is in a Columbia-0 (Col-0)
409 background. The *phyB*, *pifq*, *PIF4-OE*, *PHYB-OE* and *myc2myc4* plants were
410 generated as described previously (Wang et al., 2010; Jia et al., 2014; Ma et al., 2016;
411 Zhang et al., 2018a). The *phyBmyc2myc4* and *pifqmyc2myc4* mutant plants were
412 generated by crossing *myc2myc4* with either *phyB* or *pifq* and genotyped using
413 primers listed in **Appendix Table S2**. To generate WT/35S:MYC2-YFP and
414 *pifq/35S:MYC2-YFP* plants, MYC2 coding sequence was cloned into a pHB-X-YFP
415 vector and transferred to either WT or *pifq Arabidopsis* following the floral dip
416 method with the *Agrobacterium tumefaciens* strain GV3101(Clough and Bent, 1998).
417 Plants were grown in a phytotron with a light (fluorescent lamp, 80 $\mu\text{E/s}\cdot\text{m}^2$) /dark
418 cycle of 16 h/8 h at 22°C. For light treatment of inflorescence stem growth, plants
419 were grown under white light until bolting and transferred to various light conditions.
420 A red-light condition was achieved with a light-emitting diode (LED) light incubator
421 (Percival E30LED; 30 $\mu\text{E/s}\cdot\text{m}^2$). White light (WL; high R:FR) was provided by a WL
422 LED with a R:FR ratio of 13 (Qiding technology, 67 $\mu\text{E/s}\cdot\text{m}^2$). WL+FR (low R:FR)
423 treatment was achieved using supplementary far-red (FR) LEDs (Qiding technology,
424 47 $\mu\text{E/s}\cdot\text{m}^2$) to a R:FR ratio of 0.066. FR light was provided by FR LEDs (Qiding
425 technology, 47 $\mu\text{E/s}\cdot\text{m}^2$). All light parameters were measured with an ILT1400
426 Radiometer Photometer and an Ocean Optics HR2000+CG spectrophotometer.

427

428 **Paraffin sections**

429 Paraffin sections were performed as previously described (Zhang et al., 2018a).
430 Briefly, the basal part of the inflorescence stem was cut into a 5-mm segment and
431 fixed in FAA (Formalin-Aceto-Alcohol) solution under vacuum, stored at 4°C
432 overnight, dehydrated in a graded ethanol series, and embedded into paraffin. Samples
433 were sectioned to 10 μm thickness using a Leica RM2235 rotary microtome. The
434 sections were stained with Toluidine blue and observed under a light microscope

435 (Olympus, BX53).

436

437 **Cell wall thickness analysis**

438 The basal part of the inflorescence stem was cut into 2 mm segments, fixed in 3% (v/v)
439 paraformaldehyde and 0.5% (v/v) glutaraldehyde in PBS (0.1 M, pH 7.4), dehydrated
440 in a graded ethanol series, embedded in Epon812 and sectioned. The samples were
441 stained with 2% (w/v) uranyl acetate and lead citrate and observed under a
442 transmission electron microscope (Hitachi H-7650) as previously described (Zhao et
443 al., 2014). SCW thickness was measured with ImageJ software.

444

445 **Fiber cell length measurement**

446 The basal part of the inflorescence stem was cut into a 2 cm length and disaggregated
447 by submerging in glacial acetic acid / 30% hydrogen peroxide (v/v 1:1) solution at
448 60 °C overnight, stained with 1% safranin (w/v) for 10 min, and photographed
449 under a light microscope (Olympus, BX53). The fiber cell length was measured with
450 ImageJ software.

451

452 **RNA extraction and quantitative RT-PCR analysis**

453 Total RNA was extracted from different tissues of *Arabidopsis* plants using the
454 E.Z.N.A. Plant RNA Kit (Omega, R6827-02). The first-strand cDNA was synthesized
455 using TransScript One-Step gDNA Removal and cDNA Synthesis SuperMix
456 (TransGen Biotech, AT311-03) for quantitative real-time PCR (qRT-PCR) analysis of
457 transcript abundance. qRT-PCR was performed using SYBR Green (TransStart Tip
458 Green qPCR supermix) with a QuantStudio 3 Real-Time PCR System (Applied
459 Biosystems). Gene expression was normalized using *ACT2* as an internal control.

460

461 **Analysis of stem tensile strength and cell wall components**

462 The basal part of the inflorescence stem was used for tensile strength measurement as
463 previously described (Zhang et al., 2018a). Relative tensile strength was normalized
464 against WT. For analysis of cell wall components, the basal part of inflorescence stem

465 was collected and analysed as described by (Xi et al., 2017). Collected stems were
466 ground to a fine powder in liquid nitrogen, Alcohol-insoluble residue (AIR) was
467 obtained by successively washing the powder with 70% (v/v) ethanol,
468 chloroform/methanol (1:1 v/v), and acetone (Pettolino et al., 2012). After de-starching,
469 AIR was washed with water and acetone, and dried for lignin and crystalline cellulose
470 content determination.

471

472 **Immunoblotting**

473 Proteins extracted from seedling samples were separated with 10% (w/v) SDS-PAGE
474 gels and blotted onto polyvinylidene fluoride membrane (Bio-rad). Protein blots were
475 then analyzed using either anti-GFP/Myc (1:2000 dilution; Abmart) or anti-ACTIN
476 (1:2000 dilution; Abmart) monoclonal antibodies followed by horseradish peroxidase
477 (HRP)-conjugated goat-anti-mouse antibodies (1:5000 dilution, Thermo Fisher). Blots
478 were developed in a Tanon Imaging System (Tanon 5200CE) using ECL Western
479 Blotting Substrate (Tanon, 180-501).

480

481 **Protein subcellular localization**

482 For protein subcellular localization analyses, the MYC2/MYC4 and PIF4 coding
483 sequences were PCR-amplified with the proof-reading enzyme PHANTA (Vazyme,
484 P520) from cDNA and cloned into a pHB-X-YFP and a pHB-X-CFP vector in frame
485 with the YFP/CFP (Luo et al., 2014), respectively, and then the constructs were
486 Agro-infiltrated into *Nicotiana benthamiana* leaves according to the method of (Gui
487 et al., 2016). After incubation for 48 h in dark, abaxial epidermal cells of the leaf were
488 observed under a confocal microscope (Leica TSC SP8 STED 3X).

489

490 **Yeast two-hybrid assay**

491 The coding sequence of MYC2 PCR-amplified from cDNA using PHANTA was
492 fused with GAL4 DNA-binding domain (BD) of the bait vector pGBKT7 (Clontech).
493 N-terminal containing TAD and C-terminal containing bHLH of PIF4 were
494 PCR-amplified and fused with GAL4 activation domain (AD) of the pray vector

495 pGADT7 (Clontech). Bait and pray vectors were co-transformed in to the Y2H Gold
496 yeast strain, and then grown on SD-Trp-Leu and SD-Trp-Leu-His plates (Clontech).

497

498 **PIFs and MYC2 transcriptional activity assay**

499 The interaction of MYC2 and PIF4 activity was assayed using a dual-LUC reporter
500 assay system (Promega) through *Arabidopsis* protoplast transfection. The PIF4/ PIF5/
501 MYC2 and GFP coding sequences were cloned into the pA7 vector under the control
502 of the 35S promoter and used as an effector. The *NST1* (-1 to -3711 bp from ATG)
503 promoter sequence was cloned into *pGreenII 0800-LUC* vector upstream and in frame
504 with the luciferase (LUC) gene and was used as a reporter. Renilla luciferase (REN)
505 gene in a pGreenII0800-LUC vector was used as an internal control. Protoplasts from
506 *Arabidopsis* mesophyll cells were isolated and transformed as previously described
507 (Zhang et al., 2018a).

508

509 **Promoter GUS activity analysis**

510 The *PIF4* promoter (-1 to -4312 bp from ATG) was cloned into a pORE-R2 vector
511 (Fang et al., 2021) to drive GUS expression, then the promoter constructs were
512 transformed into wild-type *Arabidopsis* following the floral dip method (Clough and
513 Bent, 1998). Transgenic plants were selected on MS medium containing 50 µg/ml
514 hygromycin and then genotyped. Positive T2 transgenic plants were used to analyze
515 the GUS staining activity. GUS staining was conducted according to (Gui et al.,
516 2016).

517

518 **Accession Numbers**

519 Sequence data from this article can be found at <https://www.arabidopsis.org> with the
520 following accession numbers: *PHYB* (AT2G18790), *PIF1* (AT2G20180), *PIF3*
521 (AT1G09530), *PIF4* (AT2G43010), *PIF5* (AT3G59060), *MYC2* (AT1G32640),
522 *MYC4* (AT4G17880), *NST1* (AT2G46770), *SND1* (AT1G32770), *VND6*
523 (AT5G62380), *VND7* (AT1G71930), *MYB103* (AT1G63910), *CESA4* (AT5G44030),
524 *IRX8* (AT5G54690), *4CLI* (AT1G51680), *LAC4* (AT2G38080), *PER64* (AT5G42180),

525 *F5H* (AT4G36220), *PIL1* (AT2G46970), *ATHB2* (AT4G16780), *BBX28* (AT4G27310),
526 *PSY* (AT5G17230), *PORC* (AT1G03630), *GUN5* (AT5G13630), *XTH27*
527 (AT2G01850), *XTH22* (AT5G57560), *XTH30* (AT1G32170), *EXPA1* (AT1G69530)
528 and *ACT2* (AT3G18780).

529

530 **Supplemental data**

531 The following materials are available in the online version of this article.

532 **Supplemental Figure S1.** Expression of SCW-related genes under different light
533 conditions.

534 **Supplemental Figure S2.** PHYB and PIFs affect inflorescence stem properties.

535 **Supplemental Figure S3.** Phenotypes of PHYB-OE and PIF4-OE plants.

536 **Supplemental Figure S4.** Expression pattern of phyB and PIF genes.

537 **Supplemental Figure S5.** Transcriptional analysis of Arabidopsis inflorescence stem
538 treated with red light.

539 **Supplemental Figure S6.** Expression of MYC2 and SCW formation-related genes is
540 induced by red light.

541 **Supplemental Figure S7.** Far-red light inhibition MYC2 expression is dependent on
542 PHYB and PIFs.

543 **Supplemental Figure S8.** PIF4 physically interacts with MYC2.

544 **Supplemental Figure S9.** *myc2myc4* mutation rescued the phenotype of *pifq* mutant.

545 **Supplemental Table S1.** RNA-seq data of red light induced genes in 5 week old
546 inflorescence stems.

547 **Supplemental Table S2.** Primer sequences used in this study.

548

549 **Acknowledgment**

550 We thank Dr. Daoxin Xie (Tsinghua University) for providing *myc2 myc4* mutants.

551 We thank Ni Fan and Dr. Xiaoshu Gao for help on confocal microscoping. We thank

552 Xiaoyan Gao, Zhiping Zhang, Jiqin Li and Ling Ge for assistance with transmission

553 electron microscopy. This work was supported by the National Natural Science
554 Foundation of China (Grant No. 31630014) and the Chinese Academy of Sciences
555 (Grant No. XDB27020104). MSD and AB would like to acknowledge the support of
556 funds from La Trobe University and the Chinese national and provincial governments
557 to the Sino-Australia Cell Wall Research Centre, Zhejiang Agriculture and Forestry
558 University (ZAFU).

559

560 **Author contributions**

561 F.L., Q.Z., H.L., H.Y. and L.L. designed the research; F.L., Q.Z., performed the
562 experiments; F.L., Q.Z., H.L., H.Y., M.S.D., A.B. and L.L. analyzed the data; F.L.,
563 Q.Z, M.S.D. A.B. and L.L. wrote the paper. All authors read and approved the article.

564

565

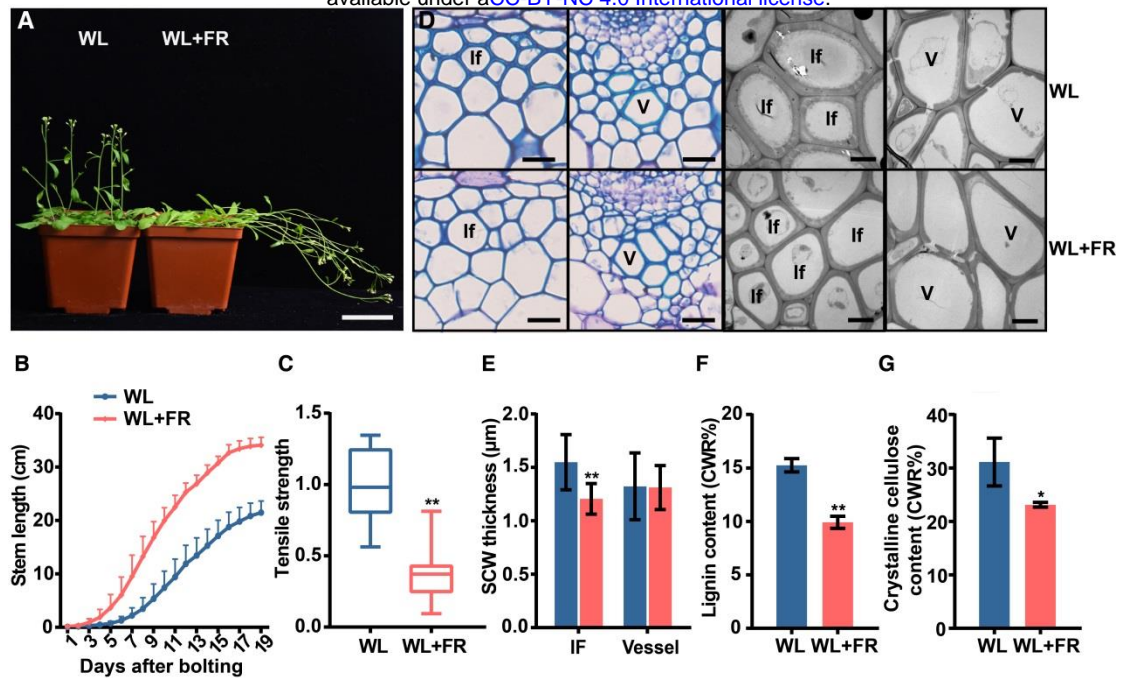


Figure 1 Shaded light inhibits SCW thickening in inflorescence stem.

A, Growth of *Arabidopsis* inflorescence stems in WL and WL+FR conditions. WL: white light. FR: far red. Scale bar = 5 cm.

B, Elongation of inflorescence stems in WL and WL+FR conditions during growth. $n = 9$, mean \pm SD.

C, Tensile strength of the inflorescence stems. Student's t test (** $P < 0.01$) was used for statistical analysis, $n = 18$, mean \pm SD.

D, Cross sections of the inflorescence stem grown under different light conditions (WL and WL+FR) visualized under the light microscope (after Toluidine blue staining; LHS panels) and the transmission electron microscope (RHS panels). If: Interfascicular fiber cell. V: Vessel cell. LHS panels: scale bar = 20 μm , RHS panels: scale bar = 5 μm .

E, Measurements of SCW thickness in the interfascicular fiber cells in (**D**). From three biological replicates, more than 10 cells were measured per biological replicate. Student's t test (** $P < 0.01$) was used for statistical analysis, mean \pm SD.

F, Lignin content in inflorescence stems of the plants grown in different R:FR conditions. Student's t test (* $P < 0.05$) was used for statistical analyses, $n = 3$, mean \pm SD.

G, Crystalline cellulose content in inflorescence stems of the plants grown in different R:FR conditions. Student's t test (* $P < 0.05$) was used for statistical analyses, $n = 3$, mean \pm SD.

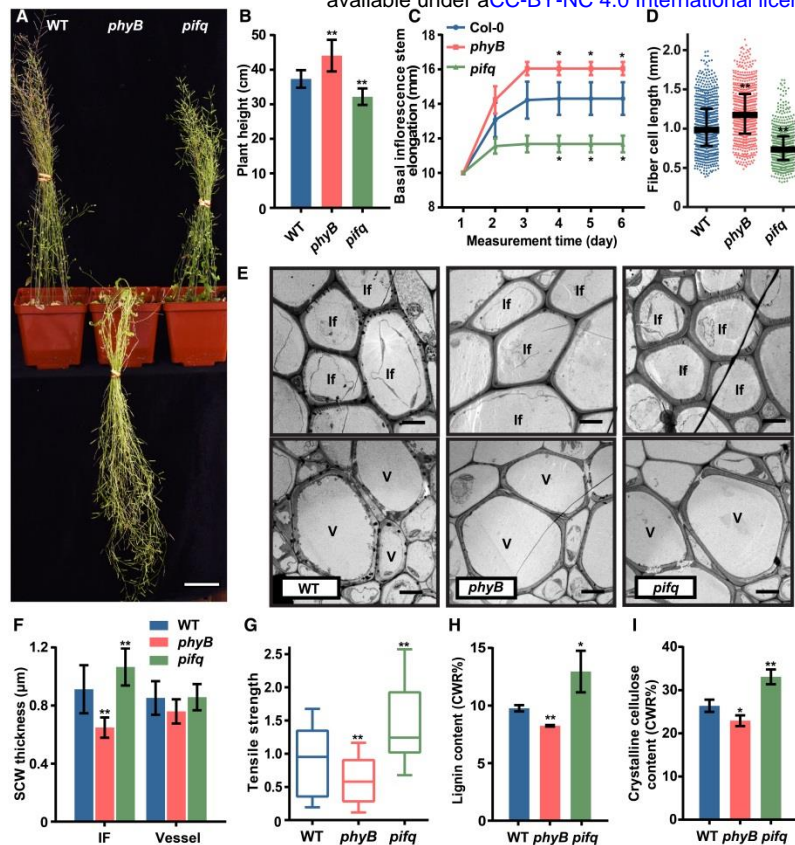


Figure 2 PHYB and PIFs regulate SCW thickening in fiber cells.

A, Plants were grown in white light (WL) at 8-weeks old. Scale bar = 5 cm.

B, Measurements of plant height in (A). Student's t test (**P < 0.01) was used for statistical analyses, n = 20, mean ± SD.

C, Inflorescence stem elongation. The stem was marked with two points at the basal region and the distance between the two points was measured every day during growth. Student's t test (*P < 0.05) was used for statistical analyses, n = 3, mean ± SD.

D, Fiber cell length measured in disaggregated fiber cells. Data were from three biological replicates and more than 200 cells were measured per biological repeats. Student's t test (**P < 0.01) was used for statistical analysis, mean ± SD.

E, Transmission electron micrographs of inflorescence stem cross-sections. If: Interfascicular fiber cell. V: Vessel cell. Scale bar = 5 μm.

F, Measurements of SCW thickness in the interfascicular fiber cells and vessel cells in (E). Data were from three biological replicates and more than 5 cells were measured per biological replicate. Student's t test (**P < 0.01) was used for statistical analysis, mean ± SD.

G, Tensile strength measurements of the inflorescence stem. Student's t test (**P < 0.01) was used for statistical analysis, n = 16, mean ± SD.

H, Lignin content in inflorescence stems. Student's t test (**P < 0.01, *P < 0.05) was used for statistical analyses, n = 3, mean ± SD.

I, Crystalline cellulose content in inflorescence stems. Student's t test (**P < 0.01, *P < 0.05) was used for statistical analyses, n = 3, mean ± SD.

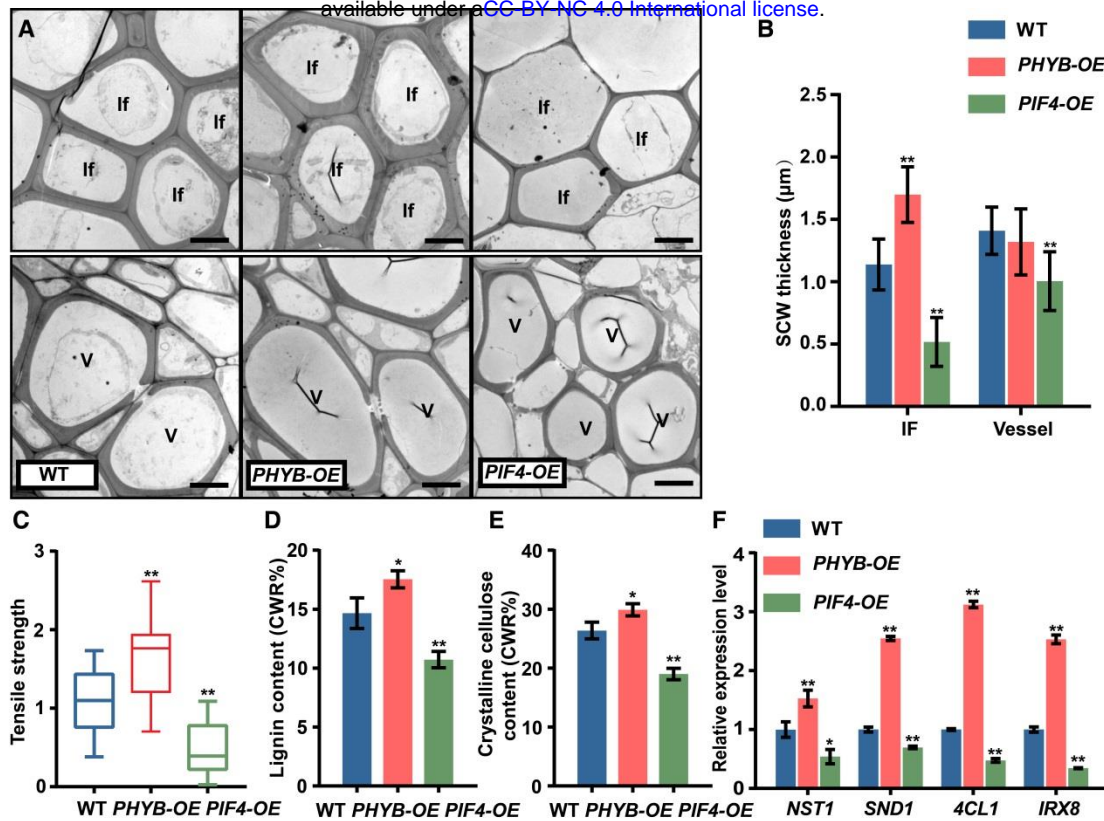


Figure 3 SCW phenotypes of *PHYB-OE* and *PIF4-OE* plants.

A, Transmission electron micrographs of inflorescence stem cross-sections. If: Interfascicular fiber cell. V: Vessel cells. Scale bar = 5 µm.

B, Measurements of SCW thickness of cells in (A). Data were from three biological replicates and more than 10 cells were measured per biological replicate. Student's t test (** $P < 0.01$) was used for statistical analysis, mean \pm SD.

C, Tensile strength of inflorescence stems. Student's t test (** $P < 0.01$) was used for statistical analysis, $n = 15$, mean \pm SD.

D, Lignin content in inflorescence stems. Student's t test (* $P < 0.05$) was used for statistical analyses, $n = 3$, mean \pm SD.

E, Cellulose content in inflorescence stems. Student's t test (** $P < 0.01$, * $P < 0.05$) was used for statistical analyses, $n = 3$, mean \pm SD.

F, Expression of SCW regulatory (*NST1* & *SND1*) and biosynthesis-related (*4CL1* & *IRX8*) genes in different genotypes grown under white light. Three biological repeats were performed. Student's t test (** $P < 0.01$, * $P < 0.05$) was used for statistical analysis, mean \pm SD.

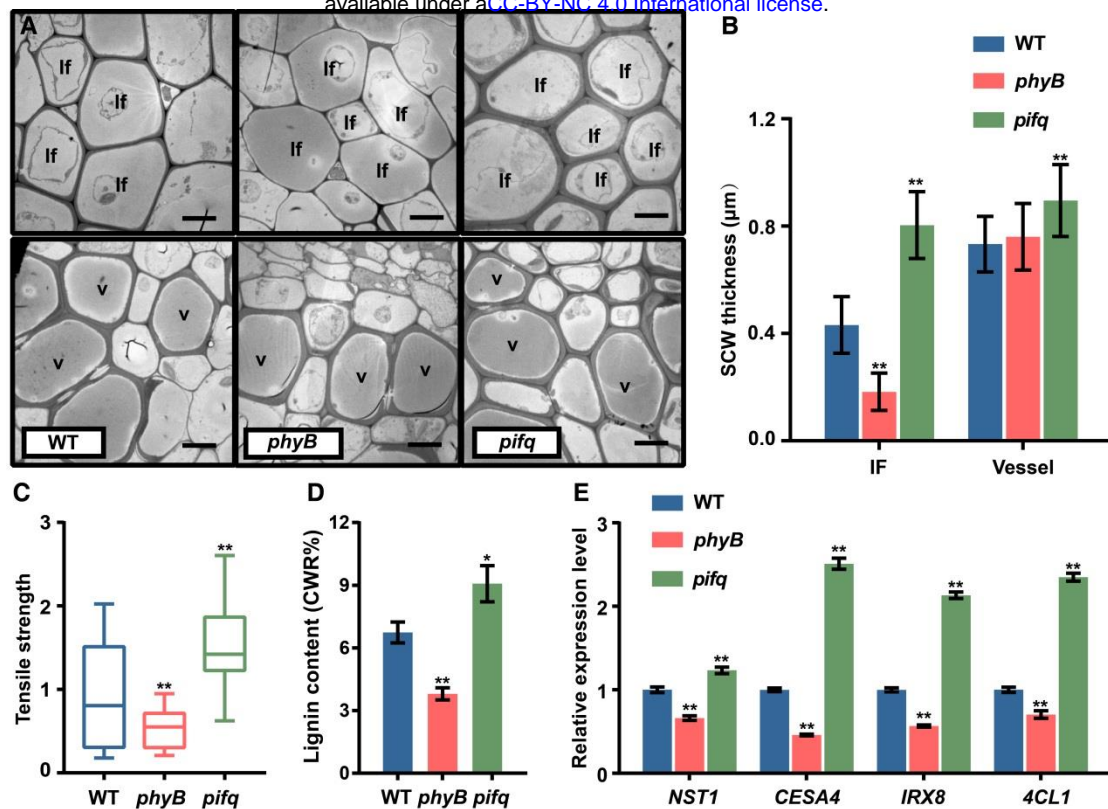


Figure 4 Red light signaling regulates SCW thickening dependent on *PHYB* and *PIFs*.

A, The inflorescence stems of *phyB* and *pifq* mutants were grown under red light (high R:FR) and anatomically analyzed. Transmission electron micrographs of the inflorescence stem cross-sections. If: Interfascicular fiber cell. V: Vessel. Scale bar = 5 μm.

B, Statistics of SCW thickness in (A). Data were three biological replicates and more than 10 cells were measured per biological replicate. Student's t test (**P < 0.01) was used for statistical analysis, mean ± SD.

C, Tensile strength of the inflorescence stem. Student's t test (**P < 0.01) was used for statistical analysis, n = 20, mean ± SD.

D, Lignin content in the inflorescence stem. Student's t test (**P < 0.01, *P < 0.05) was used for statistical analyses, n = 3, mean ± SD.

E, Expression of SCW regulatory (*NST1*) and biosynthesis-related (*CESA4*, *4CL1* & *IRX8*) was measured by qRT-PCR analysis. Three biological replicates were performed. Student's t test (**P < 0.01) was used for statistical analysis, mean ± SD.

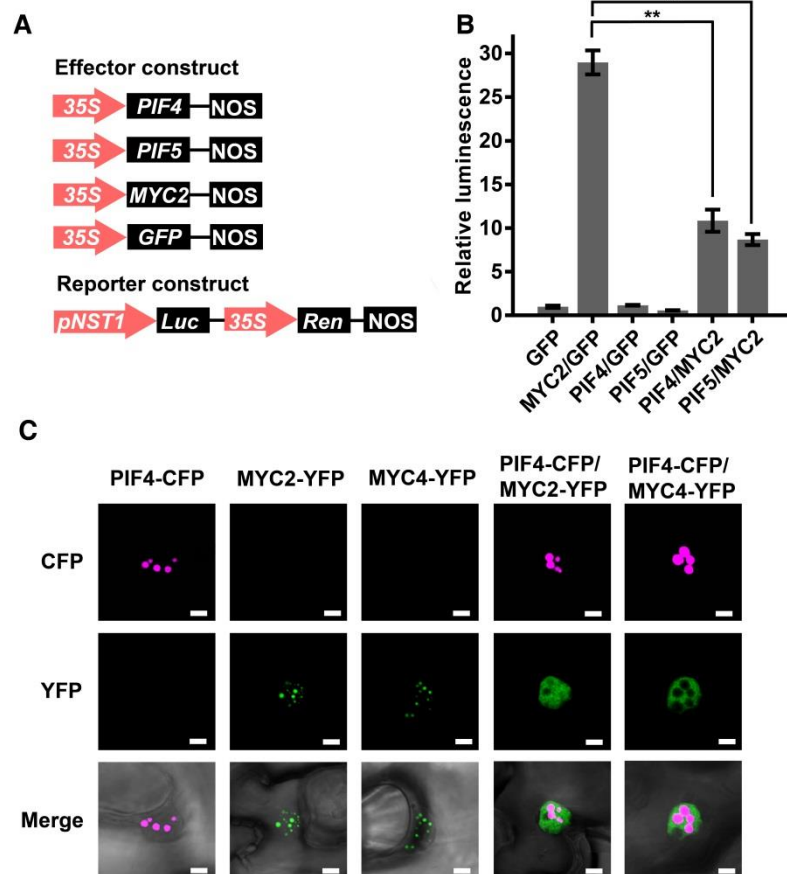


Figure 5 PIF4 represses the MYC2 transcriptional activity.

A, Schematic representation of the *NST1* promoter-driven dual-LUC reporter gene and three effector gene constructs. 35S promoter, *NST1* promoter (-1 to -3711 bp from ATG), renilla luciferase (REN), firefly luciferase (LUC) are indicated in reporter constructs. In effector constructs, PIF4, PIF5 and MYC2 are driven by the 35S promoter.

B, PIF4/PIF5 inhibit MYC2 activation of *NST1* promoter. *Arabidopsis* protoplasts were transfected with the reporter constructs in combination with different effector constructs. After transfection, the protoplasts were kept in dark for 16 h. Relative luminescence was normalized to the protoplast transformed with reporter and empty effector (GFP). Student's t test (**P < 0.01) was used for statistical analysis, n = 3, mean ± SD.

C, Subcellular localization of PIF4 and MYC2/MYC4. Constructs of PIF4-CFP, MYC2-YFP and MYC4-YFP were transferred to tobacco leaves, separately or together, by Agro-infiltration. Then the tobacco leaves were kept in dark for 12 h before fluorescence observation. Scale bar = 5 μm

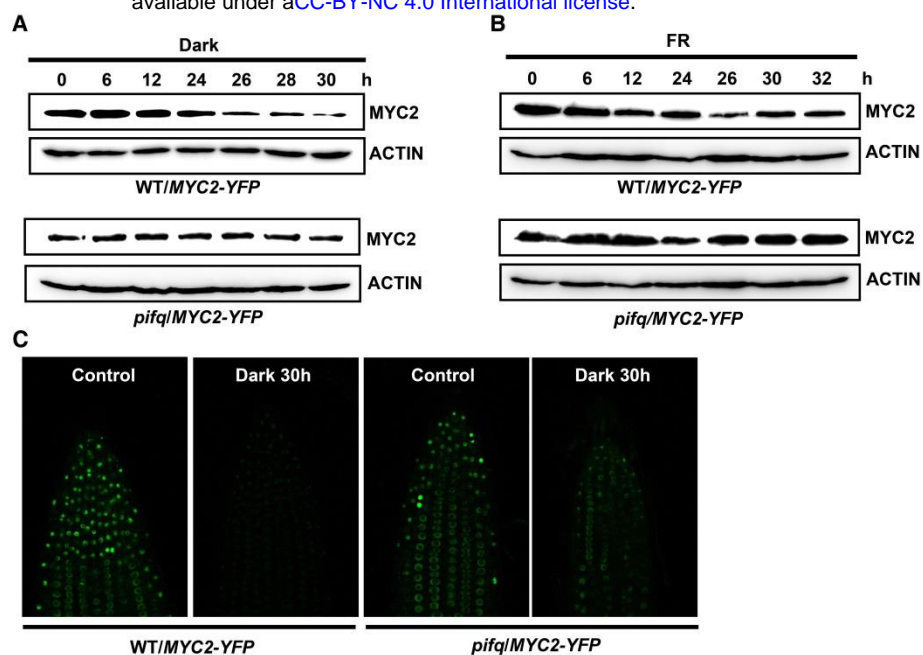


Figure 6 PIF4 affects MYC2 stability in dark and FR light.

A, Immunoblot of MYC2-YFP and ACTIN in transgenic plants. Seedlings were grown in WL condition for 10 days and then treated with dark condition. Similar results were observed in three independent experiments.

B, Immunoblot of MYC2-YFP and ACTIN in transgenic plants. Seedlings were grown in WL condition for 10 days and then treated with far-red light. Similar results were observed in three independent experiments.

C, Fluorescence signals in seedling roots. Seedlings were grown in WL condition for 4 days and then treated with/without dark for 30 h.

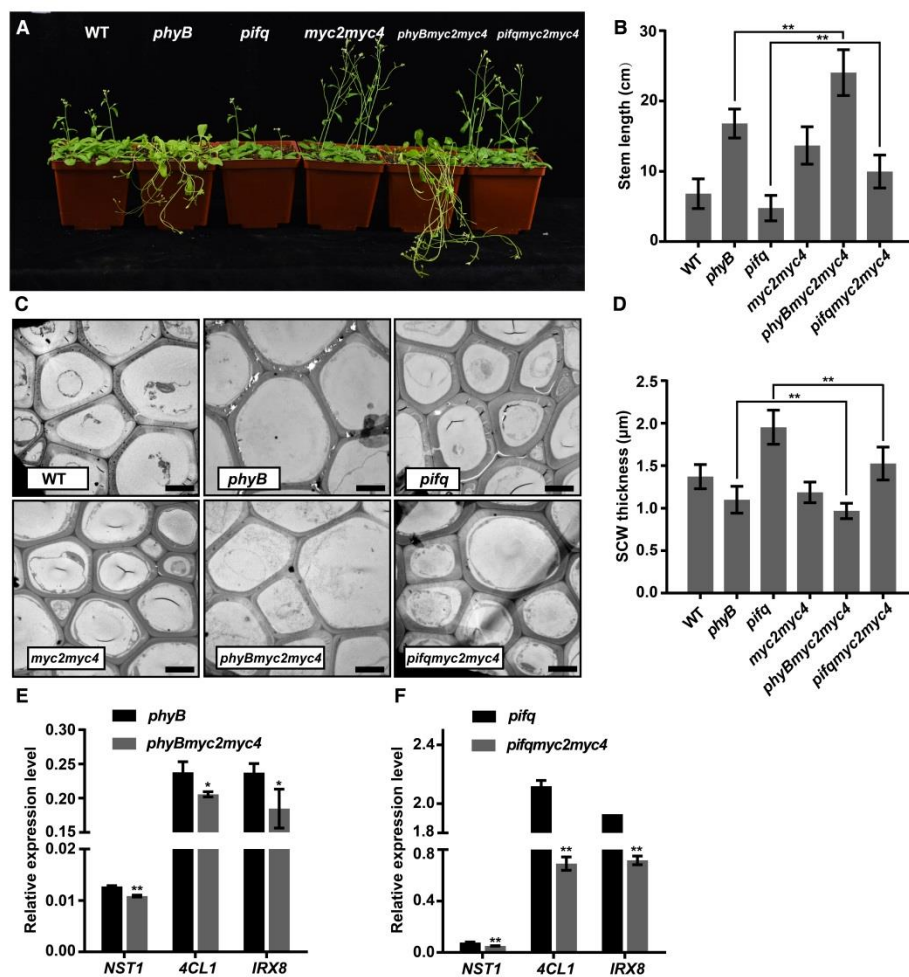


Figure 7 MYC2/MYC4 genetically interact with PIFs.

A, Mutant plants (*phyB*, *pifq*, *myc2myc4*, *phyBmyc2myc4*, *pifqmyc2myc4*) were grown in white light until 4-weeks old. Scale bar = 5 cm.

B, Inflorescence stem length in various mutants. Student's t test (**P < 0.01) was used for statistical analysis, n > 10, mean ± SD.

C, Transmission electron micrographs of stem cross sections showing interfascicular fiber cells. Scale bar = 5 μm.

D, Statistics of SCW thickness in interfascicular fiber cells in (C). Data were collected from three biological replicates and more than 10 cells were measured per biological replicate. Student's t test (**P < 0.01) was used for statistical analysis, mean ± SD.

E, F, Expression of the key SCW regulatory (*NST1*) and biosynthesis-related (*4CL1* & *IRX8*) genes in mutant plants. Three biological replicates were performed. Student's t test (**P < 0.01, *P < 0.05) was used for statistical analysis, mean ± SD.

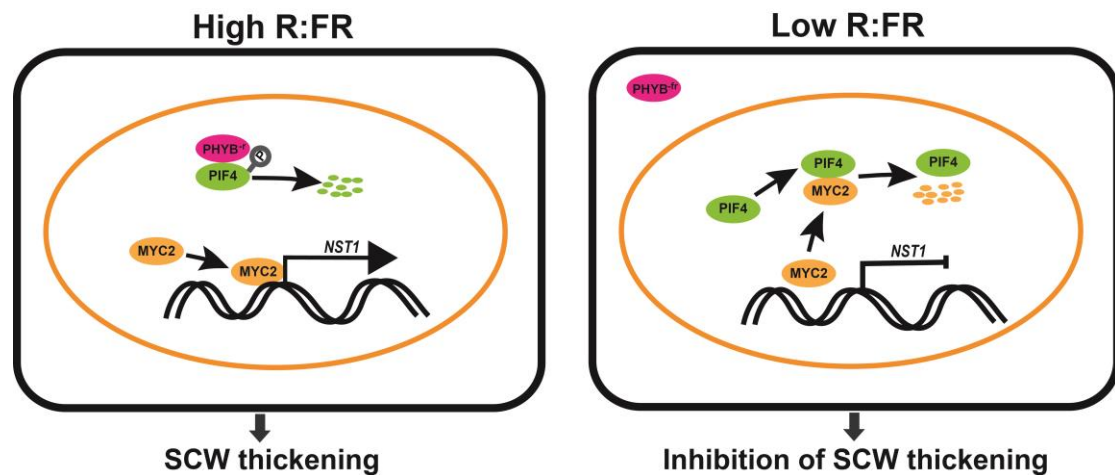


Figure 8 A proposed model of shaded light regulation of the SCW thickening.

White light enhances SCW thickening in fiber cells of inflorescence stem. Under white light (high R:FR condition), PHYB is activated to its Pfr form which enters the nucleus to inhibit PIF activity, MYC2 is available to bind to the *NST1* promoter to activate the *NST1*-direct SCW thickening process. Under shaded light (low R:FR condition), PHYB reverts to its inactive Pr form. PHYB cannot enter the nucleus and PIF proteins interact with MYC2 and displaces its binding to the *NST1* promoter. Thus, the *NST1*-directed SCW thickening process is suppressed.

Parsed Citations

- Al-Sady, B., Ni, W., Kircher, S., Schafer, E., and Quail, P.H. (2006).** Photoactivated phytochrome induces rapid PIF3 phosphorylation prior to proteasome-mediated degradation. *Mol Cell* 23, 439-446.
Google Scholar: [Author Only](#) [Title Only](#) [Author and Title](#)
- Bauer, D., Viczian, A., Kircher, S., Nobis, T., Nitschke, R., Kunkel, T., Panigrahi, K.C., Adam, E., Fejes, E., Schafer, E., and Nagy, F. (2004).** Constitutive photomorphogenesis 1 and multiple photoreceptors control degradation of phytochrome interacting factor 3, a transcription factor required for light signaling in *Arabidopsis*. *Plant Cell* 16, 1433-1445.
Google Scholar: [Author Only](#) [Title Only](#) [Author and Title](#)
- Casal, J.J. (2012).** Shade avoidance. *Arabidopsis Book* 10, e0157.
Google Scholar: [Author Only](#) [Title Only](#) [Author and Title](#)
- Chen, M., Tao, Y., Lim, J., Shaw, A., and Chory, J. (2005).** Regulation of phytochrome B nuclear localization through light-dependent unmasking of nuclear-localization signals. *Curr Biol* 15, 637-642.
Google Scholar: [Author Only](#) [Title Only](#) [Author and Title](#)
- Chen, R., Jiang, H., Li, L., Zhai, Q., Qi, L., Zhou, W., Liu, X., Li, H., Zheng, W., Sun, J., and Li, C. (2012).** The *Arabidopsis* mediator subunit MED25 differentially regulates jasmonate and abscisic acid signaling through interacting with the MYC2 and ABI5 transcription factors. *Plant Cell* 24, 2898-2916.
Google Scholar: [Author Only](#) [Title Only](#) [Author and Title](#)
- Chico, J.M., Fernandez-Barbero, G., Chini, A., Fernandez-Calvo, P., Diez-Diaz, M., and Solano, R. (2014).** Repression of Jasmonate-Dependent Defenses by Shade Involves Differential Regulation of Protein Stability of MYC Transcription Factors and Their JAZ Repressors in *Arabidopsis*. *Plant Cell* 26, 1967-1980.
Google Scholar: [Author Only](#) [Title Only](#) [Author and Title](#)
- Chico, J.M., Lechner, E., Fernandez-Barbero, G., Canibano, E., Garcia-Casado, G., Franco-Zorrilla, J.M., Hammann, P., Zamarrero, A.M., Garcia-Mina, J.M., Rubio, V., Genschik, P., and Solano, R. (2020).** CUL3(BPM) E3 ubiquitin ligases regulate MYC2, MYC3, and MYC4 stability and JA responses. *Proc Natl Acad Sci U S A* 117, 6205-6215.
Google Scholar: [Author Only](#) [Title Only](#) [Author and Title](#)
- Claisse, G., Charrier, B., and Kreis, M. (2007).** The *Arabidopsis thaliana* GSK3/Shaggy like kinase AtSK3-2 modulates floral cell expansion. *Plant Mol Biol* 64, 113-124.
Google Scholar: [Author Only](#) [Title Only](#) [Author and Title](#)
- Clough, S.J., and Bent, A.F. (1998).** Floral dip: a simplified method for *Agrobacterium*-mediated transformation of *Arabidopsis thaliana*. *The Plant Journal* 16, 735-743.
Google Scholar: [Author Only](#) [Title Only](#) [Author and Title](#)
- Didi, V., Jackson, P., and Hejatko, J. (2015).** Hormonal regulation of secondary cell wall formation. *J Exp Bot* 66, 5015-5027.
Google Scholar: [Author Only](#) [Title Only](#) [Author and Title](#)
- Doblin, M.S., Pettolino, F., and Bacic, A. (2010).** Plant cell walls: the skeleton of the plant world. *Funct Plant Biol* 37, 357-381.
Google Scholar: [Author Only](#) [Title Only](#) [Author and Title](#)
- Fang, Q., Zhou, F., Zhang, Y., Singh, S., and Huang, C.F. (2021).** STOP1 degradation mediated by the F-box proteins RAH1 and RAE1 balances aluminum resistance and plant growth in *Arabidopsis thaliana*. *Plant J*.
Google Scholar: [Author Only](#) [Title Only](#) [Author and Title](#)
- Franklin, K.A. (2008).** Shade avoidance. *New Phytol* 179, 930-944.
Google Scholar: [Author Only](#) [Title Only](#) [Author and Title](#)
- Franklin, K.A., and Quail, P.H. (2010).** Phytochrome functions in *Arabidopsis* development. *J Exp Bot* 61, 11-24.
Google Scholar: [Author Only](#) [Title Only](#) [Author and Title](#)
- Goh, H.H., Sloan, J., Dorca-Fornell, C., and Fleming, A. (2012).** Inducible repression of multiple expansin genes leads to growth suppression during leaf development. *Plant Physiol* 159, 1759-1770.
Google Scholar: [Author Only](#) [Title Only](#) [Author and Title](#)
- Gui, J., Zheng, S., Liu, C., Shen, J., Li, J., and Li, L. (2016).** OsREM4.1 Interacts with OsSERK1 to Coordinate the Interlinking between Abscisic Acid and Brassinosteroid Signaling in Rice. *Dev Cell* 38, 201-213.
Google Scholar: [Author Only](#) [Title Only](#) [Author and Title](#)
- Hao, Z., Avci, U., Tan, L., Zhu, X., Glushka, J., Pattathil, S., Eberhard, S., Sholes, T., Rothstein, G.E., Lukowitz, W., Orlando, R., Hahn, M.G., and Mohnen, D. (2014).** Loss of *Arabidopsis* GAUT12/IRX8 causes anther indehiscence and leads to reduced G lignin associated with altered matrix polysaccharide deposition. *Front Plant Sci* 5, 357.
Google Scholar: [Author Only](#) [Title Only](#) [Author and Title](#)
- Hersch, M., Lorrain, S., de Wit, M., Trevisan, M., Ljung, K., Bergmann, S., and Fankhauser, C. (2014).** Light intensity modulates the regulatory network of the shade avoidance response in *Arabidopsis*. *Proc Natl Acad Sci U S A* 111, 6515-6520.
Google Scholar: [Author Only](#) [Title Only](#) [Author and Title](#)

- Hong, G.J., Xue, X.Y., Mao, Y.B., Wang, L.J., and Chen, X.Y. (2012). Arabidopsis MYC2 interacts with DELLA proteins in regulating sesquiterpene synthase gene expression. *Plant Cell* 24, 2635-2648.
Google Scholar: [Author Only](#) [Title Only](#) [Author and Title](#)
- Hori, C., Yu, X., Mortimer, J., Sano, R., Matsumoto, T., Kikuchi, J., Demura, T., and Ohtani, M. (2020). Impact of abiotic stress on the regulation of cell wall biosynthesis in *Populus trichocarpa*. *Plant Biotechnology* 37.
Google Scholar: [Author Only](#) [Title Only](#) [Author and Title](#)
- Hornitschek, P., Kohnen, M.V., Lorrain, S., Rougemont, J., Ljung, K., Lopez-Vidriero, I., Franco-Zorrilla, J.M., Solano, R., Trevisan, M., Pradervand, S., Xenarios, I., and Fankhauser, C. (2012). Phytochrome interacting factors 4 and 5 control seedling growth in changing light conditions by directly controlling auxin signaling. *Plant J* 71, 699-711.
Google Scholar: [Author Only](#) [Title Only](#) [Author and Title](#)
- Huang, C., Zhang, R., Gui, J., Zhong, Y., and Li, L. (2018). The Receptor-Like Kinase AtVRLK1 Regulates Secondary Cell Wall Thickening. *Plant Physiol* 177, 671-683.
Google Scholar: [Author Only](#) [Title Only](#) [Author and Title](#)
- Jang, I.C., Henriques, R., Seo, H.S., Nagatani, A., and Chua, N.H. (2010). Arabidopsis PHYTOCHROME INTERACTING FACTOR proteins promote phytochrome B polyubiquitination by COP1 E3 ligase in the nucleus. *Plant Cell* 22, 2370-2383.
Google Scholar: [Author Only](#) [Title Only](#) [Author and Title](#)
- Jia, K.-P., Luo, Q., He, S.-B., Lu, X.-D., and Yang, H.-Q. (2014). Strigolactone-Regulated Hypocotyl Elongation Is Dependent on Cryptochrome and Phytochrome Signaling Pathways in Arabidopsis. *Molecular Plant* 7, 528-540.
Google Scholar: [Author Only](#) [Title Only](#) [Author and Title](#)
- Jia, Y., Kong, X., Hu, K., Cao, M., Liu, J., Ma, C., Guo, S., Yuan, X., Zhao, S., Robert, H.S., Li, C., Tian, H., and Ding, Z. (2020). PIFs coordinate shade avoidance by inhibiting auxin repressor ARF18 and metabolic regulator QQS. *New Phytol* 228, 609-621.
Google Scholar: [Author Only](#) [Title Only](#) [Author and Title](#)
- Jung, C., Zhao, P., Seo, J.S., Mitsuda, N., Deng, S., and Chua, N.H. (2015). PLANT U-BOX PROTEIN10 Regulates MYC2 Stability in Arabidopsis. *Plant Cell* 27, 2016-2031.
Google Scholar: [Author Only](#) [Title Only](#) [Author and Title](#)
- Kazan, K., and Manners, J.M. (2013). MYC2: The Master in Action. *Molecular Plant* 6, 686-703.
Google Scholar: [Author Only](#) [Title Only](#) [Author and Title](#)
- Kozuka, T., Kobayashi, J., Horiguchi, G., Demura, T., Sakakibara, H., Tsukaya, H., and Nagatani, A. (2010). Involvement of Auxin and Brassinosteroid in the Regulation of Petiole Elongation under the Shade. *Plant Physiology* 153, 1608-1618.
Google Scholar: [Author Only](#) [Title Only](#) [Author and Title](#)
- Le Gall, H., Philippe, F., Domon, J.M., Gillet, F., Pelloux, J., and Rayon, C. (2015). Cell Wall Metabolism in Response to Abiotic Stress. *Plants (Basel)* 4, 112-166.
Google Scholar: [Author Only](#) [Title Only](#) [Author and Title](#)
- Lee, D., Meyer, K., Chapple, C., and Douglas, C.J. (1997). Antisense suppression of 4-coumarate:coenzyme A ligase activity in Arabidopsis leads to altered lignin subunit composition. *Plant Cell* 9, 1985-1998.
Google Scholar: [Author Only](#) [Title Only](#) [Author and Title](#)
- Leivar, P., and Quail, P.H. (2011). PIFs: pivotal components in a cellular signaling hub. *Trends Plant Sci* 16, 19-28.
Google Scholar: [Author Only](#) [Title Only](#) [Author and Title](#)
- Leivar, P., and Monte, E. (2014). PIFs: systems integrators in plant development. *Plant Cell* 26, 56-78.
Google Scholar: [Author Only](#) [Title Only](#) [Author and Title](#)
- Leivar, P., Tepperman, J.M., Cohn, M.M., Monte, E., Al-Sady, B., Erickson, E., and Quail, P.H. (2012). Dynamic antagonism between phytochromes and PIF family basic helix-loop-helix factors induces selective reciprocal responses to light and shade in a rapidly responsive transcriptional network in Arabidopsis. *Plant Cell* 24, 1398-1419.
Google Scholar: [Author Only](#) [Title Only](#) [Author and Title](#)
- Liu, Y., Jafari, F., and Wang, H. (2021). Integration of light and hormone signaling pathways in the regulation of plant shade avoidance syndrome. *aBIOTECH*.
Google Scholar: [Author Only](#) [Title Only](#) [Author and Title](#)
- Lorrain, S., Allen, T., Duek, P.D., Whitlam, G.C., and Fankhauser, C. (2008). Phytochrome-mediated inhibition of shade avoidance involves degradation of growth-promoting bHLH transcription factors. *Plant J* 53, 312-323.
Google Scholar: [Author Only](#) [Title Only](#) [Author and Title](#)
- Lucas, W.J., Groover, A., Lichtenberger, R., Furuta, K., Yadav, S.R., Helariutta, Y., He, X.Q., Fukuda, H., Kang, J., Brady, S.M., Patrick, J.W., Sperry, J., Yoshida, A., Lopez-Millan, A.F., Grusak, M.A., and Kachroo, P. (2013). The plant vascular system: evolution, development and functions. *J Integr Plant Biol* 55, 294-388.
Google Scholar: [Author Only](#) [Title Only](#) [Author and Title](#)
- Luo, Q., Lian, H.L., He, S.B., Li, L., Jia, K.P., and Yang, H.Q. (2014). COP1 and phyB Physically Interact with PIL1 to Regulate Its Stability

and Photomorphogenic Development in Arabidopsis. *Plant Cell* 26, 2441-2456.

Google Scholar: [Author Only Title Only Author and Title](#)

Ma, D., Li, X., Guo, Y., Chu, J., Fang, S., Yan, C., Noel, J.P., and Liu, H. (2016). Cryptochrome 1 interacts with PIF4 to regulate high temperature-mediated hypocotyl elongation in response to blue light. *Proc Natl Acad Sci U S A* 113, 224-229.

Google Scholar: [Author Only Title Only Author and Title](#)

Matsui, A., Yokoyama, R., Seki, M., Ito, T., Shinozaki, K., Takahashi, T., Komeda, Y., and Nishitani, K. (2005). AtXTH27 plays an essential role in cell wall modification during the development of tracheary elements. *Plant J* 42, 525-534.

Google Scholar: [Author Only Title Only Author and Title](#)

McCahill, I.W., and Hazen, S.P. (2019). Regulation of Cell Wall Thickening by a Medley of Mechanisms. *Trends Plant Sci* 24, 853-866.

Google Scholar: [Author Only Title Only Author and Title](#)

Mitsuda, N., Iwase, A., Yamamoto, H., Yoshida, M., Seki, M., Shinozaki, K., and Ohme-Takagi, M. (2007). NAC transcription factors, NST1 and NST3, are key regulators of the formation of secondary walls in woody tissues of Arabidopsis. *Plant Cell* 19, 270-280.

Google Scholar: [Author Only Title Only Author and Title](#)

Monte, E., Tepperman, J.M., Al-Sady, B., Kaczorowski, K.A., Alonso, J.M., Ecker, J.R., Li, X., Zhang, Y., and Quail, P.H. (2004). The phytochrome-interacting transcription factor, PIF3, acts early, selectively, and positively in light-induced chloroplast development. *Proc. Natl. Acad. Sci. USA* 101, 16091-16098.

Google Scholar: [Author Only Title Only Author and Title](#)

Ortigosa, A., Fonseca, S., Franco-Zorrilla, J.M., Fernandez-Calvo, P., Zander, M., Lewsey, M.G., Garcia-Casado, G., Fernandez-Barbero, G., Ecker, J.R., and Solano, R. (2020). The JA-pathway MYC transcription factors regulate photomorphogenic responses by targeting HY5 gene expression. *Plant J* 102, 138-152.

Google Scholar: [Author Only Title Only Author and Title](#)

Pedmale, U.V., Huang, S.C., Zander, M., Cole, B.J., Hetzel, J., Ljung, K., Reis, P.A.B., Sridevi, P., Nito, K., Nery, J.R., Ecker, J.R., and Chory, J. (2016). Cryptochromes Interact Directly with PIFs to Control Plant Growth in Limiting Blue Light. *Cell* 164, 233-245.

Google Scholar: [Author Only Title Only Author and Title](#)

Pettolino, F.A., Walsh, C., Fincher, G.B., and Bacic, A. (2012). Determining the polysaccharide composition of plant cell walls. *Nat Protoc* 7, 1590-1607.

Google Scholar: [Author Only Title Only Author and Title](#)

Pham, V.N., Kathare, P.K., and Huq, E. (2018). Phytochromes and Phytochrome Interacting Factors. *Plant physiology* 176, 1025-1038.

Google Scholar: [Author Only Title Only Author and Title](#)

Quail, P.H. (1991). PHYTOCHROME: A Light-activated Molecular Switch that Regulates Plant Gene Expression. *Annual Review of Genetics* 25, 389-409.

Google Scholar: [Author Only Title Only Author and Title](#)

Reed, J.W., Nagpal, P., Poole, D.S., Furuya, M., and Chory, J. (1993). Mutations in the gene for the red/far-red light receptor phytochrome B alter cell elongation and physiological responses throughout Arabidopsis development. *The Plant Cell* 5, 147.

Google Scholar: [Author Only Title Only Author and Title](#)

Sasidharan, R., Chinnappa, C.C., Voesenek, L.A.C.J., and Pierik, R. (2008). The Regulation of Cell Wall Extensibility during Shade Avoidance: A Study Using Two Contrasting Ecotypes of *Stellaria longipes*. *Plant Physiol* 148, 1557-1569.

Google Scholar: [Author Only Title Only Author and Title](#)

Sasidharan, R., Chinnappa, C.C., Staal, M., Elzenga, J.T., Yokoyama, R., Nishitani, K., Voesenek, L.A., and Pierik, R. (2010). Light quality-mediated petiole elongation in Arabidopsis during shade avoidance involves cell wall modification by xyloglucan endotransglucosylase/hydrolases. *Plant Physiol* 154, 978-990.

Google Scholar: [Author Only Title Only Author and Title](#)

Shen, Y., Khanna, R., Carle, C.M., and Quail, P.H. (2007). Phytochrome induces rapid PIF5 phosphorylation and degradation in response to red-light activation. *Plant Physiol* 145, 1043-1051.

Google Scholar: [Author Only Title Only Author and Title](#)

Song, S., Huang, H., Gao, H., Wang, J., Wu, D., Liu, X., Yang, S., Zhai, Q., Li, C., Qi, T., and Xie, D. (2014). Interaction between MYC2 and ETHYLENE INSENSITIVE3 modulates antagonism between jasmonate and ethylene signaling in Arabidopsis. *Plant Cell* 26, 263-279.

Google Scholar: [Author Only Title Only Author and Title](#)

Strasser, B., Sanchez-Lamas, M., Yanovsky, M.J., Casal, J.J., and Cerdan, P.D. (2010). Arabidopsis thaliana life without phytochromes. *Proc Natl Acad Sci U S A* 107, 4776-4781.

Google Scholar: [Author Only Title Only Author and Title](#)

Taylor-Teeples, M., Lin, L., de Lucas, M., Turco, G., Toal, T.W., Gaudinier, A., Young, N.F., Trabucco, G.M., Veling, M.T., Lamothe, R., Handakumbura, P.P., Xiong, G., Wang, C., Corwin, J., Tsoukalas, A., Zhang, L., Ware, D., Pauly, M., Kliebenstein, D.J., Dehesh, K., Tagkopoulos, I., Breton, G., Pruneda-Paz, J.L., Ahnert, S.E., Kay, S.A., Hazen, S.P., and Brady, S.M. (2015). An Arabidopsis gene regulatory network for secondary cell wall synthesis. *Nature* 517, 571-575.

Google Scholar: [Author Only Title Only Author and Title](#)

Toledo-Ortiz, G., Johansson, H., Lee, K.P., Bou-Torrent, J., Stewart, K., Steel, G., Rodriguez-Concepcion, M., and Halliday, K.J. (2014). The HY5-PIF regulatory module coordinates light and temperature control of photosynthetic gene transcription. *PLoS Genet* 10, e1004416.

Google Scholar: [Author Only Title Only Author and Title](#)

Wang, F.F., Lian, H.L., Kang, C.Y., and Yang, H.Q. (2010). Phytochrome B is involved in mediating red light-induced stomatal opening in *Arabidopsis thaliana*. *Mol Plant* 3, 246-259.

Google Scholar: [Author Only Title Only Author and Title](#)

Withers, J., Yao, J., Mecey, C., Howe, G.A., Melotto, M., and He, S.Y. (2012). Transcription factor-dependent nuclear localization of a transcriptional repressor in jasmonate hormone signaling. *Proceedings of the National Academy of Sciences* 109, 20148.

Google Scholar: [Author Only Title Only Author and Title](#)

Wu, L., Zhang, W., Ding, Y., Zhang, J., Cambula, E.D., Weng, F., Liu, Z., Ding, C., Tang, S., Chen, L., Wang, S., and Li, G. (2017). Shading Contributes to the Reduction of Stem Mechanical Strength by Decreasing Cell Wall Synthesis in Japonica Rice (*Oryza sativa* L.). *Front Plant Sci* 8, 881.

Google Scholar: [Author Only Title Only Author and Title](#)

Xi, W., Song, D., Sun, J., Shen, J., and Li, L. (2017). Formation of wood secondary cell wall may involve two type cellulose synthase complexes in *Populus*. *Plant Mol Biol* 93, 419-429.

Google Scholar: [Author Only Title Only Author and Title](#)

Yadav, V., Mallappa, C., Gangappa, S.N., Bhatia, S., and Chattopadhyay, S. (2005). A basic helix-loop-helix transcription factor in *Arabidopsis*, MYC2, acts as a repressor of blue light-mediated photomorphogenic growth. *Plant Cell* 17, 1953-1966.

Google Scholar: [Author Only Title Only Author and Title](#)

Yamaguchi, M., Goue, N., Igarashi, H., Ohtani, M., Nakano, Y., Mortimer, J.C., Nishikubo, N., Kubo, M., Katayama, Y., Kakegawa, K., Dupree, P., and Demura, T. (2010). VASCULAR-RELATED NAC-DOMAIN6 and VASCULAR-RELATED NAC-DOMAIN7 effectively induce transdifferentiation into xylem vessel elements under control of an induction system. *Plant Physiol* 153, 906-914.

Google Scholar: [Author Only Title Only Author and Title](#)

Zhang, Q., Xie, Z., Zhang, R., Xu, P., Liu, H., Yang, H., Doblin, M.S., Bacic, A., and Li, L. (2018a). Blue Light Regulates Secondary Cell Wall Thickening via MYC2/MYC4 Activation of the NST1-Directed Transcriptional Network in *Arabidopsis*. *Plant Cell* 30, 2512-2528.

Google Scholar: [Author Only Title Only Author and Title](#)

Zhang, X., Ji, Y., Xue, C., Ma, H., Xi, Y., Huang, P., Wang, H., An, F., Li, B., Wang, Y., and Guo, H. (2018b). Integrated Regulation of Apical Hook Development by Transcriptional Coupling of EIN3/EIL1 and PIFs in *Arabidopsis*. *Plant Cell* 30, 1971-1988.

Google Scholar: [Author Only Title Only Author and Title](#)

Zhang, Y., Mayba, O., Pfeiffer, A., Shi, H., Tepperman, J., Speed, T., and Quail, P. (2013). A Quartet of PIF bHLH Factors Provides a Transcriptionally Centered Signaling Hub That Regulates Seedling Morphogenesis through Differential Expression-Patterning of Shared Target Genes in *Arabidopsis*. *PLoS Genetics* 9, e1003244.

Google Scholar: [Author Only Title Only Author and Title](#)

Zhao, P., Zhang, X., Gong, Y., Wang, D., Xu, D., Wang, N., Sun, Y., Gao, L., Liu, S.S., Deng, X.W., Kliebenstein, D.J., Zhou, X., Fang, R.X., and Ye, J. (2021). Red-light is an environmental effector for mutualism between begomovirus and its vector whitefly. *PLoS Pathog* 17, e1008770.

Google Scholar: [Author Only Title Only Author and Title](#)

Zhao, Y., Sun, J., Xu, P., Zhang, R., and Li, L. (2014). Intron-mediated alternative splicing of WOOD-ASSOCIATED NAC TRANSCRIPTION FACTOR1B regulates cell wall thickening during fiber development in *Populus* species. *Plant Physiol* 164, 765-776.

Google Scholar: [Author Only Title Only Author and Title](#)

Zhong, R., and Ye, Z.H. (2015). Secondary cell walls: biosynthesis, patterned deposition and transcriptional regulation. *Plant Cell Physiol* 56, 195-214.

Google Scholar: [Author Only Title Only Author and Title](#)

Zhong, R., Demura, T., and Ye, Z.H. (2006). SND1, a NAC domain transcription factor, is a key regulator of secondary wall synthesis in fibers of *Arabidopsis*. *Plant Cell* 18, 3158-3170.

Google Scholar: [Author Only Title Only Author and Title](#)

Zhong, R., Lee, C., and Ye, Z.H. (2010). Global analysis of direct targets of secondary wall NAC master switches in *Arabidopsis*. *Mol Plant* 3, 1087-1103.

Google Scholar: [Author Only Title Only Author and Title](#)

Zhong, R., Lee, C., Zhou, J., McCarthy, R.L., and Ye, Z.H. (2008). A battery of transcription factors involved in the regulation of secondary cell wall biosynthesis in *Arabidopsis*. *Plant Cell* 20, 2763-2782.

Google Scholar: [Author Only Title Only Author and Title](#)